Available online at www.sciencedirect.com
SCIENCE DIRECT®
PERGAMON
Control Engineering Practice 11 (2003) 531–540
CONTROL ENGINEERING PRACTICE
www.elsevier.com/locate/conengprac

Lateral control of a backward driven front-steering vehicle

R. Rajamani*, C. Zhu, L. Alexander

Department of Mechanical Engineering, University of Minnesota, 111 Church Street SE, Minneapolis, MN 55414, USA

Received 5 April 2001; accepted 14 July 2002

Abstract

This paper addresses control of the lateral position and orientation of a backward driven front steering vehicle. The low speed associated with backward driving eliminates some challenges but introduces others in lateral control design. While slip angles are small and can be neglected, other small angle approximations can no longer be made. The curvature of the desired path can be very sharp requiring large steering angles. Two control strategies based on a nonlinear kinematic model of the vehicle are developed. One controller is based on input-state feedback linearization with no associated internal dynamics. The other controller incorporates preview and is based on input–output linearization with stable internal dynamics. A major portion of the paper concentrates on experimental implementation of the two controllers using an instrumented Navistar truck. The experimental performance on straight and circular paths as well as on transient curved paths is studied. Good experimental performance is obtained with a spacing accuracy better than 40 cm being achieved in the worst case transient paths. The use of preview turns out to be important with the preview-incorporating controller providing superior performance.

Keywords: Lateral vehicle control; Steering control; Backward driving; GPS; Automated parking

1. Introduction

There are several low speed applications where vehicles need to be driven backwards. For instance, cargo vehicles (such as lift trucks) have to travel among crowded areas in a warehouse. Often there is inadequate space to turn around so that the vehicle has to move backwards in a maneuver similar to parallel parking. A similar application is the automated maneuvering of trucks in crowded freight depots. Vehicles also have to be driven backwards during parallel parking.

The last few years have seen a tremendous amount of research in the area of vehicle automation and automated highway systems. The steering control system for forward driving has been studied extensively in literature and demonstrated experimentally by several researchers (Ackermann, Guldner, Sienel, Steinhauser, & Utkin (1995); Alexander & Donath, 1999; Hingwe & Tomizuka, 1997; Hessburg, Peng, Tomizuka, Zhang, & Kamei, 1991; Peng & Tomizuka, 1993; Tan, Guldner, Chen, & Patwardhan, 1998; Pham, Hedrick, & Tomizuka, 1994 and Chen & Tomizuka, 1997). The lateral control systems developed and experimentally implemented include the frequency shaped linear quadratic (FSLQ) controller with preview (Peng & Tomizuka, 1993), linear controllers using "virtual look-ahead" by using front and rear position measurements (Tan et al., 1998) and controllers designed using a nonlinear system approach (Pham et al., 1994; Hingwe & Tomizuka, 1997 and Chen & Tomizuka, 1997).

Compared with forward driving, backward driving control has received much less attention. Previous work on lateral control during backward driving has been reported by Patwardhan et al. (1997), Kim and Oh (1999) and Guanrong and Delin (1997). Patwardhan et al. (1997) developed a control design approach based on the observation of the kinematic similarity of a boat with rudder and the car driven backwards. Guanrong and Delin (1997) used a fuzzy logic approach to design a controller for tracking sub-optimal distance trajectories with a backward driving truck.

The backward traveling direction and its associated low speed eliminate some challenges but introduce others in lateral control design problem. If the lateral

*Corresponding author. Tel.: +1-612-626-7961; fax: +1-612-625-4344.
E-mail address: rajamani@me.umn.edu (R. Rajamani).

0967-0661/02/$ - see front matter
PII: S0967-0661(02)00143-0

position is sensed at the front of the vehicle (as is typical) while the vehicle travels backward, then the vehicle dynamics constitute a non-minimum phase system. This problem is addressed in this paper by using estimated yaw-angle to project lateral displacement measurement to the back of the vehicle. The yaw-angle is estimated using an observer that utilizes gyroscope and GPS measurements. An additional challenge is that the curvature of the desired path can be very sharp requiring large steering angles. A nonlinear control strategy that utilizes a nonlinear kinematic vehicle model and incorporates preview is therefore used in developing the control system.

2. Lateral vehicle model

Researchers working with automated vehicle control have typically used linear dynamic models for the lateral motion control problem. However, for purposes of the low speed operation described in this paper, a nonlinear kinematic model is more suitable to describe the dynamics of the vehicle.

A kinematic model of the vehicle motion while it is driven backwards can be obtained by analyzing the geometric relation in Fig. 1. We assume that there is no sideslip at any of the tires (i.e. the velocity angle at each tire is the same as the steering angle of the tire):

$$\dot{x} = V\cos\psi, \tag{1}$$

$$\dot{y} = V\sin\psi, \tag{2}$$

$$\dot{\psi} = -\frac{V\tan\delta}{L}, \tag{3}$$

where L is the distance between the front and rear tires (wheelbase) and V is the longitudinal velocity. Note that the equations are written in terms of the global coordinates x, y and ψ, not in body-fixed coordinates. The velocity V is typically obtained from a model of the longitudinal dynamics of the vehicle. For purposes of this paper, we will assume that V is measured and known.

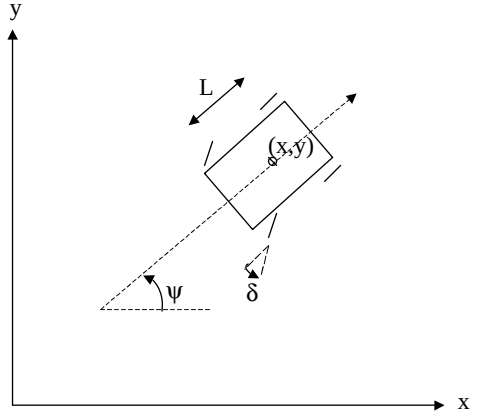

Fig. 1. Vehicle with 3° of freedom.

3. Steering control design using input-state feedback linearization

The objective of the lateral control system is to ensure that the lateral position error y_b and the vehicle orientation ψ both track desired values. The lateral position error here is defined as the distance from the vehicle e.g. to the road center measured perpendicular to the vehicle (see Fig. 3). Define the tracking errors in x and y as

$$e_{1y} = y - y_{des}, \tag{4}$$

$$e_{1x} = x - x_{des}. \tag{5}$$

Then the lateral position error is related to e_{1y} and e_{1x} as follows

$$y_b\cos\psi = e_{1y}, \tag{6a}$$

$$y_b\sin\psi = e_{1x}. \tag{6b}$$

Define the vehicle orientation error as

$$e_2 = \psi - \psi_{des}. \tag{7}$$

Let us assume that the desired trajectory has been defined, so that y_{des}, x_{des} and ψ_{des} are defined.

In this section, we develop an input-state feedback linearization control law based on controlling either the variable y or the variable x to desired values. Considering δ as the control input, the relative degree of the system is two with either x or y as outputs. Consider the problem of ensuring that y tracks y_{des}. We have

$$\ddot{y}_{des} = \left[\frac{\mathrm{d}}{\mathrm{d}t}(v\sin\psi)\right]_{des} = V\dot{\psi}_{des}\cos\psi_{des} + \dot{V}\sin\psi_{des} \tag{8}$$

and

$$\ddot{y} = \dot{\psi}V\cos(\psi) + \dot{V}\sin(\psi)$$

$$= -\frac{V^2}{L}\tan(\delta)\cos(\psi) + \dot{V}\sin(\psi). \tag{9}$$

Subtracting (8) from (9), we get

$$\ddot{e}_{1y} = -\frac{V^2}{L}\tan\delta\cos\psi + \dot{V}\sin\psi - V\dot{\psi}_{des}\cos\psi_{des} - \dot{V}\sin\psi_{des}. \tag{10}$$

Designing the controller to be:

$$\delta = \tan^{-1}\left[-\frac{L}{V^2\cos\psi}(V\dot{\psi}_{des}\cos\psi_{des} + \dot{V}\sin\psi_{des} - \dot{V}\sin\psi - \lambda_1\dot{e}_{1y} - \lambda_2 e_{1y})\right] \tag{11a}$$

we obtain the closed-loop dynamics as

$$\ddot{e}_{1y} = -\lambda_1 \dot{e}_{1y} - \lambda_2 e_{1y}$$

ensuring that as $t \to \infty$, $e_{1y} \to 0$ and $\dot{e}_{1y} \to 0$ i.e. $y \to y_{des}$.

If V is constant, the control law simplifies to

$$\delta = \tan^{-1}\left\{ -\frac{L\cos(\psi_{des})}{V \cos\psi}\dot{\psi}_{des} + \frac{L}{V^2\cos(\psi)}(-\lambda_1 \dot{e}_{1y} - \lambda_2 e_{1y})\right\}. \quad (11b)$$

The control law (11a) is valid only if $\psi \neq \pm\pi/2$. Indeed for the case where $\psi = \pm\pi/2$, y becomes equivalent to the vehicle longitudinal position and can therefore no longer be controlled using the steering input δ. In this case, one could control x to its desired value. The following control law that ensures that x tracks its desired value can be obtained similar to Eq. (11a)

$$\delta = \tan^{-1}\left[\frac{L}{V^2 \sin\psi}(-V\dot{\psi}_{des}\sin\psi_{des} + \dot{V}\cos\psi_{des} - \dot{V}\cos\psi - \lambda_1 \dot{e}_{1x} - \lambda_2 e_{1x})\right]. \quad (12a)$$

If V is constant, the control law (12a) simplifies to

$$\delta = \tan^{-1}\left\{ -\frac{L}{V}\frac{\sin(\psi_{des})}{\sin(\psi)}\dot{\psi}_{des} + \frac{L}{V^2\sin(\psi)}(-\lambda_1 \dot{e}_{1x} - \lambda_2 e_{1x})\right\}. \quad (12b)$$

Fig. 2 describes the regions in the $x-y$ plane where Eqs. (11a), (11b) and (12) are to be used for control respectively. We thus choose between x-control and y-control depending on the region of operation in the $x-y$ plane.

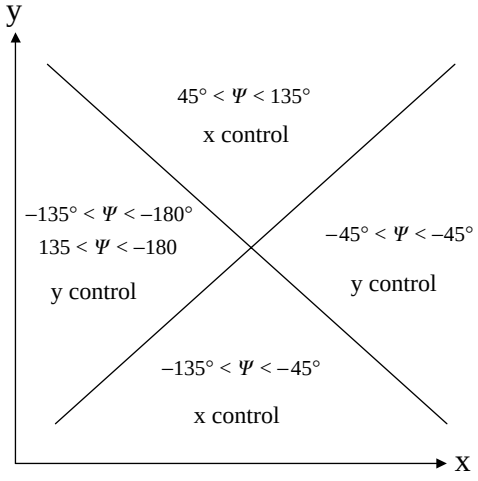

Fig. 2. x-control and y-control regions.

Note that at the boundaries between the x-control and y-control regions, the error values e_{1x} and e_{1y} and their derivatives are both continuous. To see this, note that $\sin\psi = \cos\psi$ at each of the boundaries. Hence $e_{1x} = e_{1y}$. Also

$$\dot{y}_b = \frac{\dot{e}_{1y}}{\cos\psi} + \frac{\sin\psi}{\cos^2\psi}\dot{\psi}e_{1y} = \frac{\dot{e}_{1x}}{\sin\psi} - \frac{\cos\psi}{\sin^2\psi}\dot{\psi}e_{1x}.$$

Again, since $\sin\psi = \cos\psi$ at the boundaries, we have $\dot{e}_{1x} = \dot{e}_{1y}$.

Now let us analyze the convergence of the state variable ψ. Since there are no internal dynamics in the system, the variable ψ is guaranteed to remain bounded with the above controller. To find the steady state value of ψ, note that the ψ dynamics using (11b) are given by

$$\dot{\psi} = -\frac{V\tan\delta}{L}$$

$$= -\frac{V}{L}\left[-\frac{L}{V}\frac{\cos(\psi_{des})}{\cos(\psi)}\dot{\psi}_{des} + \frac{1}{V^2\cos\psi}(-\lambda_1\dot{e}_{1y} - \lambda_2 e_{1y})\right]$$

$$= \frac{\cos(\psi_{des})}{\cos(\psi)}\dot{\psi}_{des} - \frac{1}{LV\cos\psi}(-\lambda_1\dot{e}_{1y} - \lambda_2 e_{1y}).$$

Since $e_{1y} \to 0$ and $\dot{e}_{1y} \to 0$, we have $\dot{\psi}\cos(\psi) \to \dot{\psi}_{des}\cos(\psi_{des})$. This implies $\mathrm{d}/\mathrm{d}t(\sin\psi) \to d/\mathrm{d}t(\sin\psi_{des})$. Also, the convergence property $\dot{y} \to \dot{y}_{des}$ implies $V(\sin\psi - \sin\psi_{des}) \to 0$. Hence $\psi \to \psi_{des}$.

The above control law can be changed to implement lateral control for low-speed forward vehicle motion by simply changing the sign in Eqs. (11a), (11b) and (12).

4. Input–output feedback linearization with preview

The control law in Section 3 was found in experiments to work well while tracking a straight line. While on a circular road, or on a transient between a straight line and a circular road, it could not meet performance objectives.

A new control law based on input–output feedback linearization with incorporation of preview from a map is developed. Unlike the input-state feedback linearization law, this control law has unobservable internal dynamics. However, the internal dynamics are stable.

Define $z = y_b + l^*(e_2 + \psi_d - \psi_{pd}/2)$. This is to be interpreted as the previewed lateral distance from vehicle to road center, see Fig. 3. Here y_b is the present lateral distance from vehicle to road center calculated perpendicular to the vehicle body and ψ_{pd} is the previewed desired yaw rate. Let $\alpha = \psi_d - \psi_{pd}/2$. α will be zero if the trajectory is a straight line.

Setting $\dot{z} = -\lambda z$, we get

$$\dot{y}_b + l\left(\dot{e}_2 + \frac{\dot{\psi}_d - \dot{\psi}_{pd}}{2}\right) = -\lambda z$$

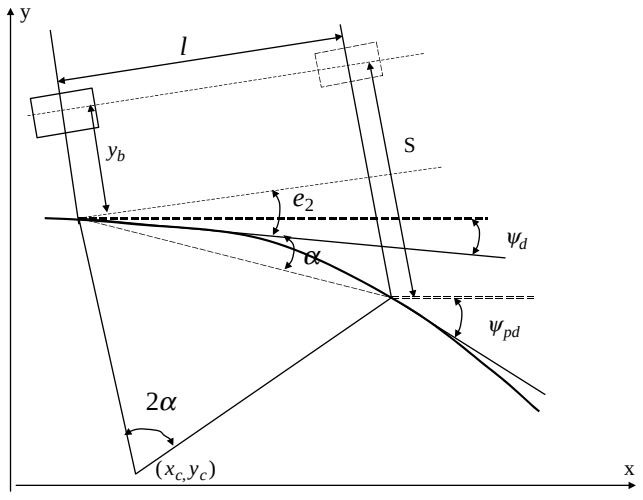

Fig. 3. Improved preview control algorithm.

and substituting for $\dot{e}_2 = \dot{\psi} - \dot{\psi}_{des}$, we obtain the steering controller as

$$\delta = -\frac{L}{lv}\tan^{-1} \times \left(-\lambda y_b - \lambda l * e_2 - \lambda\frac{\psi_d - \psi_{pd}}{2} - \dot{y}_b + \frac{(\dot{\psi}_d + \dot{\psi}_{pd})l}{2}\right). \quad (13)$$

Here ψ_d and $\dot{\psi}_d$ are feed forward information from map. ψ_{pd} and $\dot{\psi}_{pd}$ are the preview road information ahead of the vehicle. It is easy to show that for this preview control law, $z \to 0$ as $t \to \infty$. The above controller law shows satisfactory performance on both straight lines and curves.

The preview control law can be used for control during forward driving simply by switching the sign in Eq. (13).

Since the relative degree of the above system is 1, the stability of the internal dynamics needs to be analyzed. Considering the coordinate ψ to represent the internal dynamics, we find

$$\dot{\psi} = -\frac{V}{L}\tan(\delta) = -\lambda\psi + \lambda\psi_{des} - \frac{\lambda(\psi_d - \psi_{pd})}{2} + \ell\frac{(\dot{\psi}_d + \dot{\psi}_{pd})}{2}. \quad (14)$$

Hence the internal dynamics are seen to be input-state stable. If ψ_{des} is constant (as in a straight road) then $\dot{\psi} = -\lambda\psi + \lambda\psi_{des}$ and in this case the vehicle orientation ψ converges to the road orientation ψ_{des}.

5. Experimental implementation

5.1. Experimental hardware

The "Safetruck" is a Navistar International 9400 tractor-trailer used by researchers at the ITS-Institute, University of Minnesota, to conduct research on various highway vehicle automation technologies. The truck is equipped with a Novatel RT-20 GPS system aided by differential correction. The GPS system provides the position of the truck to an accuracy of 2.5 cm at an update rate of 200 ms. In addition, an Andrews fiber-optic gyroscope that measures the yaw rate of the truck and an Analog Devices MEMS accelerometer that measures lateral acceleration are available. A potentiometer on the steering wheel column is used to measure the steering angle. An Eaton Vorad EVT300 radar is mounted just above the front bumper of the truck. It can simultaneously measure distance, relative velocity and azimuth angle to as many as 12 different targets on the highway. The truck is also equipped with steering, throttle and brake actuators for automatic control. RT Kernel on a PC laptop serves as the real-time software platform.

A photograph of the Safetruck is shown in Fig. 4. Though the figure shows a tractor-trailer, only the tractor was used for the experimental work in this particular project.

5.2. Calculation of y_b using GPS

Next we will study how to calculate the lateral displacement error based on GPS signals and road map information. A map of the road was constructed as a simple list of points spaced every 1 m apart. Each point information included x, y coordinates, the desired yaw angle and the curvature at that point. For a given vehicle position, we need to find out the lateral distance between vehicle and the desired trajectory based on these points.

The lateral error of the vehicle, as shown in Fig. 5, satisfies the following equation

$$\tan(-\psi) = \frac{x - x_r}{y - y_r}, \quad (15)$$

where (x, y) is the vehicle position and $(x_r y_r)$ is the desired vehicle position.

If the trajectory between the map points is considered as a straight line, the trajectory satisfies the equation

$$\frac{x_r - x_{r1}}{y_r - y_{r1}} = \frac{x_{r2} - x_{r1}}{y_{r2} - y_{r1}}, \quad (16)$$

where $(x_{r1} y_{r1})$ and $(x_{r2} y_{r2})$ are points from the map. The two Eqs. (15) and (16) can be solved for (x_r, y_r). Once (x_r, y_r) is obtained, the lateral error is given by the distance between the points (x_r, y_r) and (x, y).

The absolute value of the lateral displacement error can then be represented as

$$|y_b| = \sqrt{(x - x_r)^2 + (y - y_r)^2}.$$

Fig. 4. Navistar 9400 tractor-trailer.

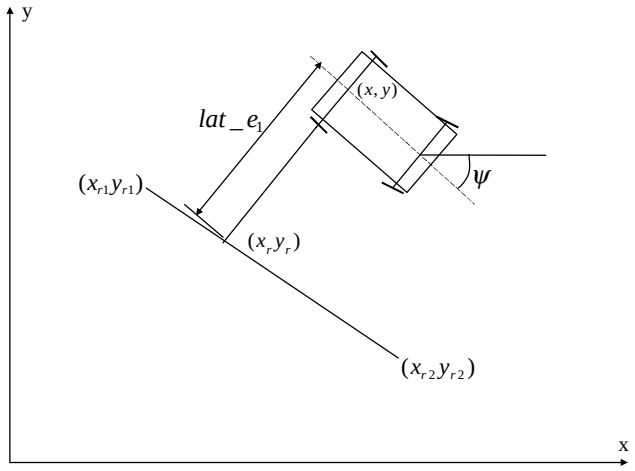

Fig. 5. Lateral displacement calculation on straight line.

From the analysis shown in Fig. 6, it can be concluded that the lateral displacement error as a whole can be expressed as

$$y_b = \text{sign}(y - y_r) * \text{sign}(\cos\psi)\sqrt{(x - x_r)^2 + (y - y_r)^2} \tag{17}$$

5.3. Obtaining e_2 from an observer

The yaw angle of the vehicle can be obtained from GPS signals using

$$\psi_{GPS} = \tan^{-1}\left(\frac{\dot{y}}{\dot{x}}\right). \tag{18}$$

However, $\dot{y}$ and $\dot{x}$ both have to be obtained by numerical differentiation making this a very noisy signal. The yaw angle can also be obtained by integrating the yaw-rate signal measured by a gyroscope $\dot{\psi}_{gyro}$. However, the signal obtained by integration of the yaw-rate usually drifts due to bias errors present in the yaw-rate signal.

The following observer that utilizes both the gyroscope and GPS is therefore used to obtain ψ:

$$\dot{\hat{\psi}} = \dot{\psi}_{gyro} + k(\psi_{GPS} - \hat{\psi}). \tag{19}$$

Here the term $\psi_{GPS} - \hat{\psi}$ corrects for the drift that occurs when the gyroscope signal $\dot{\psi}_{gyro}$ is integrated. If the gyroscope signal were perfect with no bias errors, then there would be no drift and the use of GPS would be unnecessary. A very small value of k leads to a slow correction in drift but a smoother signal. A high value of k leads to quicker correction of drift but a noisier estimate.

6. Experimental performance

6.1. Steering control on a straight road

The input-state linearization controller described in Section 3 has good performance along a straight road. The experimental performance corresponding to initial condition errors of lateral displacement –0.5 m and initial yaw error 10° is shown in Fig. 7. The steady state lateral displacement from the centerline is seen to be within ± 0.15 m. The steady state yaw error is less than 2°. However, the transient response time is rather slow, with a rise time of the order of 2.5 s.

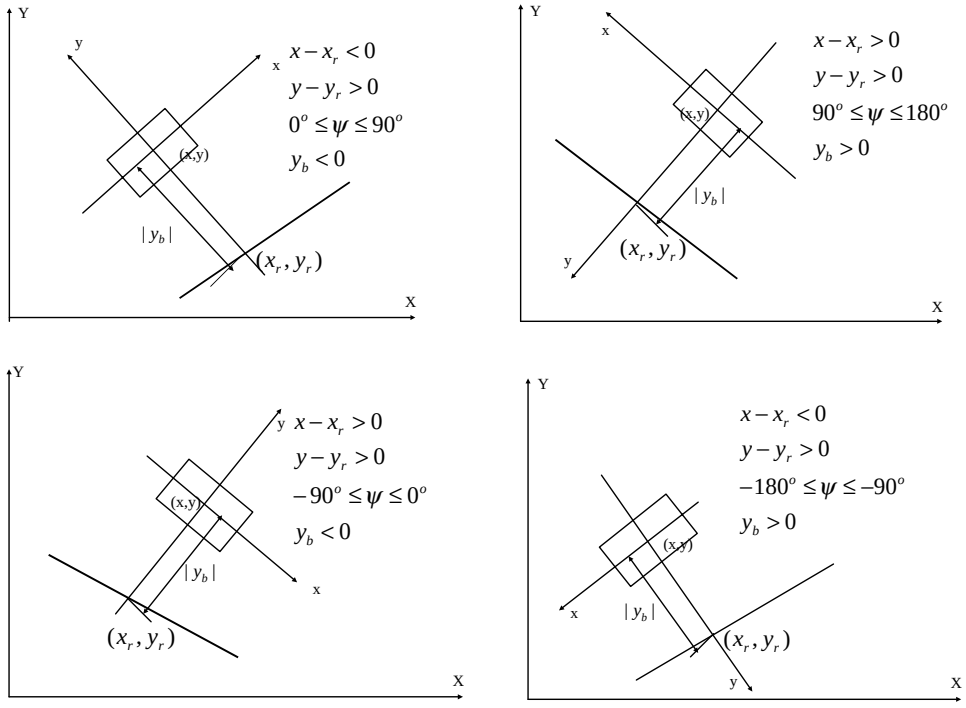

Fig. 6. Sign of lateral displacement.

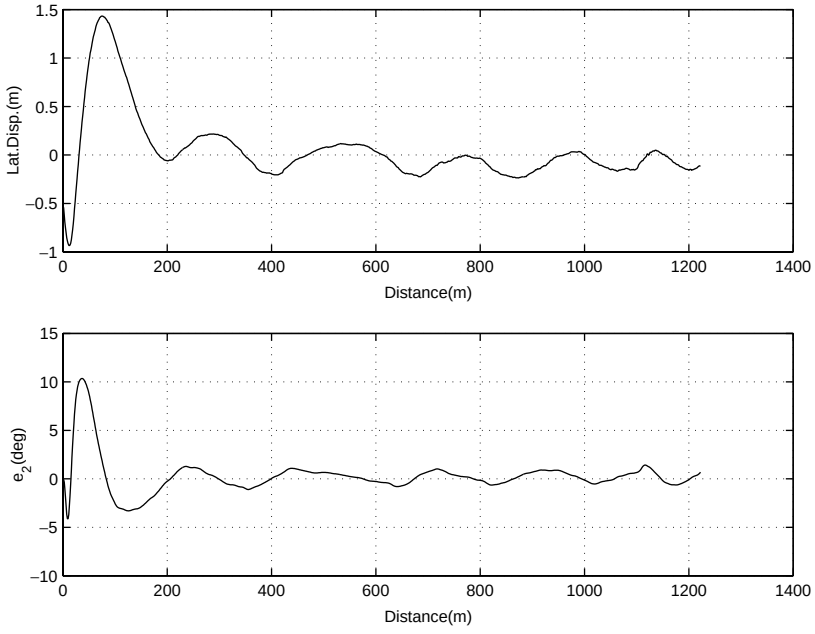

Fig. 7. Lane following performance along straight road without preview.

Instead of controlling $y_b \to 0$, we next control the preview point to be zero as discussed in Section 4. The performance is improved in three ways. First, there is more damping and less oscillation in the system. Second, the steady state lateral error is ± 0.10 m which is smaller than the controller without preview. And third, the system response is faster compared to the first case. The experimental performance with the preview controller is shown in Fig. 8.

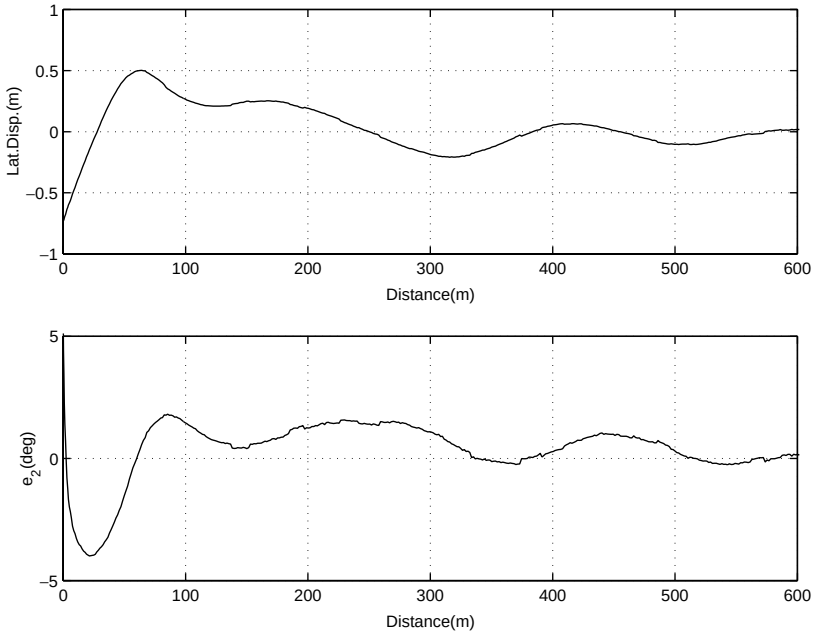

Fig. 8. Lane following performance along the straight road with preview.

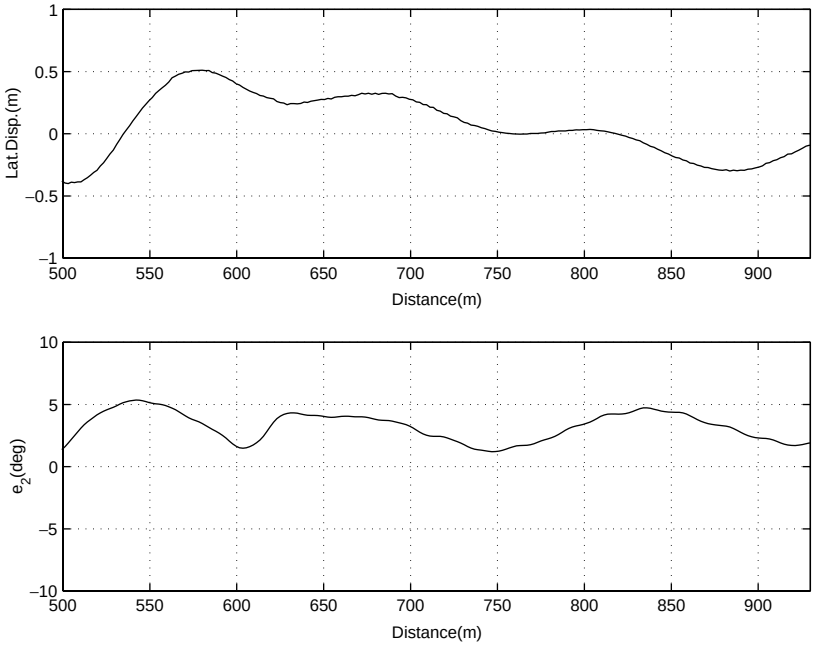

Fig. 9. Lane following performance along curve without preview.

6.2. Steering performance on a curved road

The experimental response of the lateral control system with the vehicle driving along a curve of constant radius (starting from a non-zero initial error) is studied. The closed loop system response with the non-preview controller is shown in Fig. 9. Fig. 10 shows the corresponding experimental trajectory and desired trajectory. The maximum lateral displacement error is seen to be 0.4 m.

The close loop system response is improved substantially when preview is added to the controller, as shown in Fig. 11. The overall maximum error is within ± 0.30 m. The yaw error is bounded and its maximum value is less than 4°.

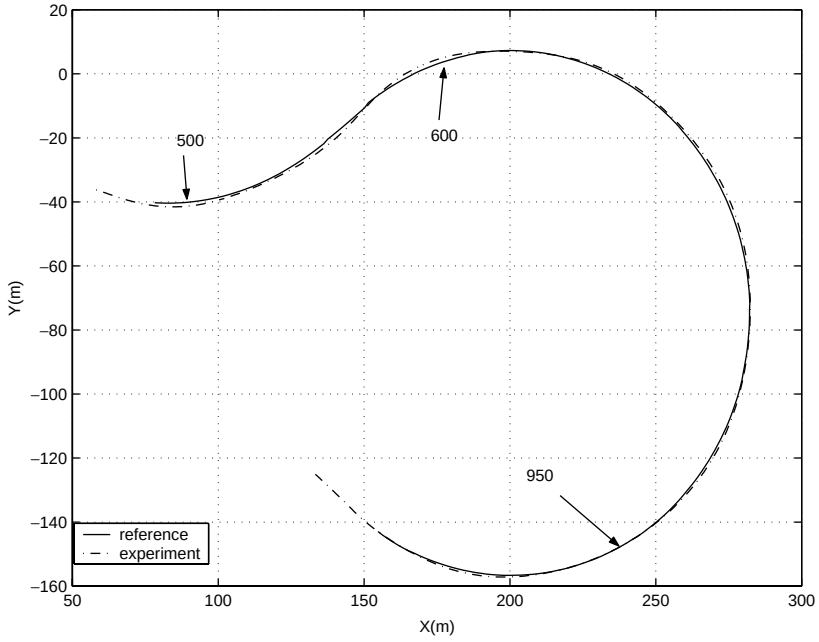

Fig. 10. Experimental trajectory and the desired trajectory of curve test.

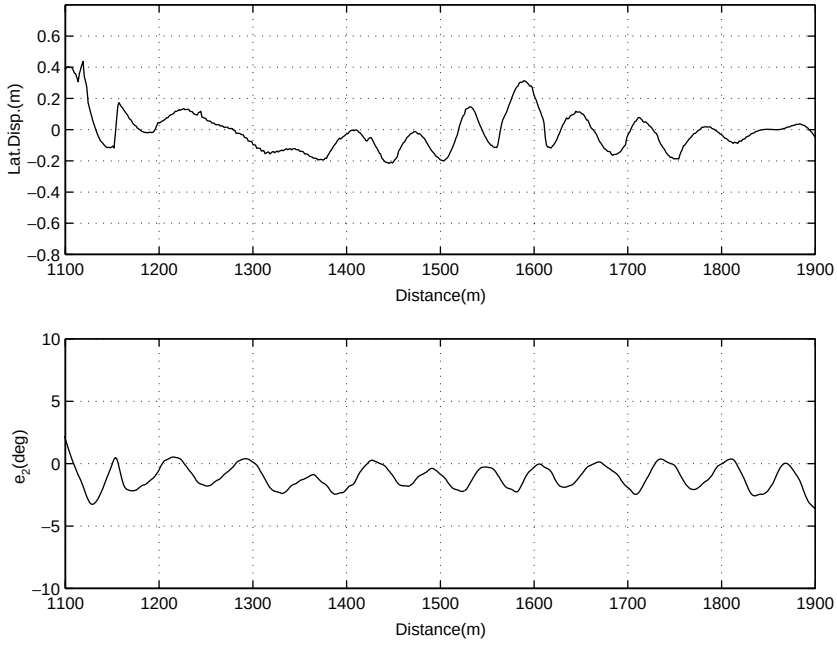

Fig. 11. Lane following performance along curve with preview.

6.3. Transient response

In a typical parallel parking task, the desired trajectory essentially consists of two straight lines and two curves with opposite curvature. The response over the transient between the straight line and curve or the transient between the two opposite curves, is important to the success of the parallel parking maneuver. The experimental performance of the preview lateral controller over transient parking-like maneuvers is shown in Figs. 12 and 13. From Fig. 12, it can be seen that an error performance within ± 0.4 m is achieved. Fig. 13 shows the desired trajectory and the actual experimental trajectory achieved.

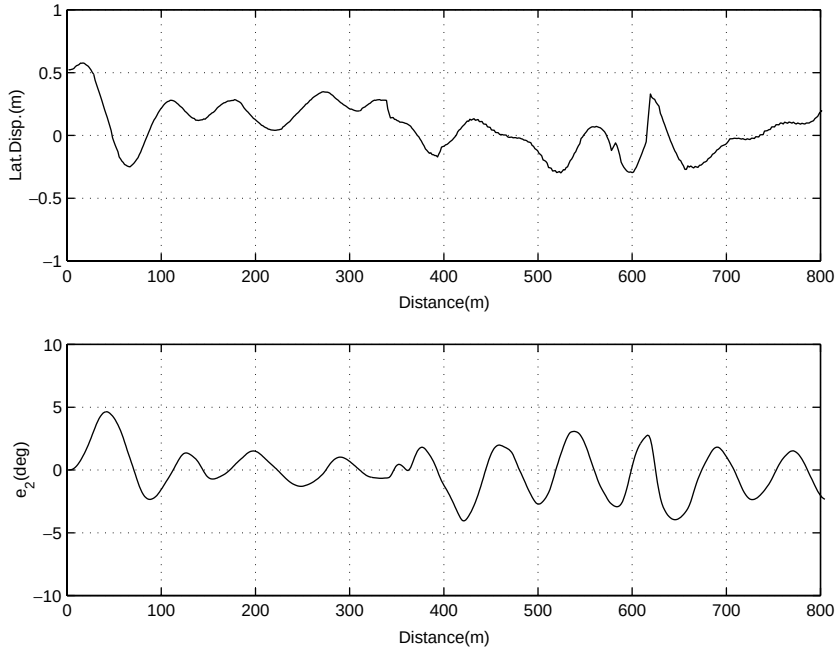

Fig. 12. Lane following performance along the transient section with preview.

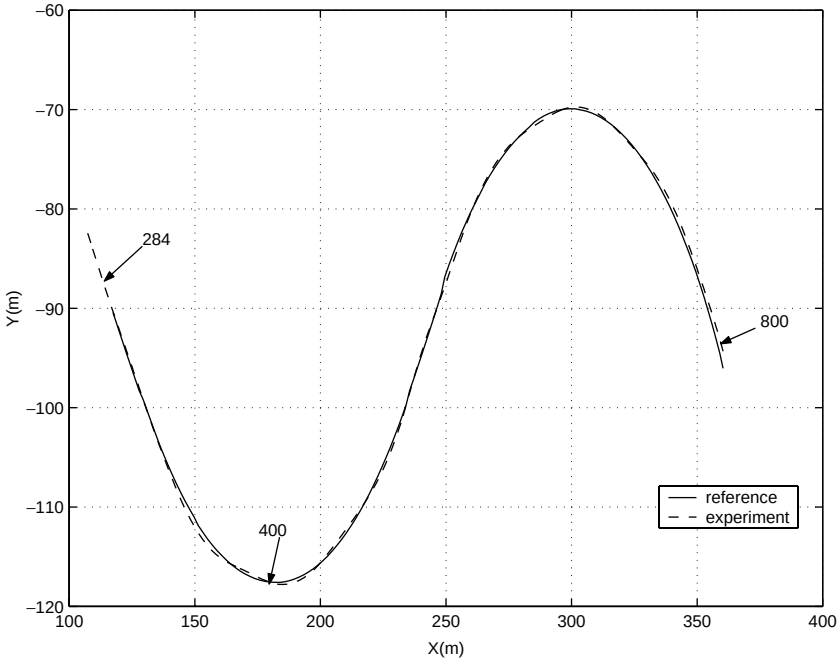

Fig. 13. Experimental and desired trajectory for transient road test.

7. Conclusions

Two control strategies based on a nonlinear kinematic model of the vehicle were developed for control of the lateral position and orientation of a backward driven front steering vehicle. One controller was based on input-state feedback linearization with no associated internal dynamics. The other controller incorporated preview and was based on input–output linearization with stable internal dynamics. A major portion of the paper concentrated on experimental implementation of the two controllers using an instrumented Navistar

truck. The experimental performance on straight and circular paths as well as on transient curved paths was studied. Good experimental performance was obtained with a spacing accuracy better than 40 cm being achieved in the worst case transient paths. The use of preview turned out to be important with the preview-incorporating controller providing superior performance. The differential GPS system provided position updates at 5 Hz. Obtaining faster position updates can lead to performance improvements.

References

Ackermann, J., Guldner, J., Sienel, W., Steinhauser, R., & Utkin, B. (1995). Linear and nonlinear controller design for robust automatic Steering. *IEEE Transactions on Control Systems Technology*, *3*(1), 132–142.

Alexander, L., & Donath, M. (1999). Differential GPS based control of a heavy vehicle. *Proceeding of the IEEE/IEEJ/JSAI international conference on intelligent transportation systems* (pp. 662–7), Tokyo, Japan.

Chen, C., Tomizuka, M. (1997). Vehicle lateral control on automated highways: A backstepping approach. *Proceedings of the IEEE conference on decision and control*, San Diego, CA, USA.

Guanrong, C., & Delin, Z. (1997). Back-driving a truck with suboptimal distance trajectories: A fuzzy logic control approach. *IEEE Transactions on Fuzzy Systems*, *5*(3), 369–380.

Hessburg, T., Peng, H., Tomizuka, M., Zhang, B.-B., & Kamei, E. (1991). An experimental study on lateral control of a vehicle. *Proceedings of the American Control Conference*, *3*, 3084–3089.

Hingwe, P., & Tomizuka, M. (1997). Experimental evaluation of a chatter free sliding mode control for lateral control in AHS. *Proceeding of the American Control Conference*, Vol. 5 (97CH36041, pp. 3365–3369). Piscataway, NJ, USA: IEEE.

Kim, D.-H., & Oh, J.-H. (1999). Experiments of backward tracking for trailer system. *Proceedings of the IEEE International Conference on Robotics and Automation*, *1*, 19–22.

Patwardhan, S., Tan, H. S., Guldner, J., & Tomizuka, M. (1997). Lane following during backward driving for front wheel steered vehicles. *Proceeding of the American control conference*, Albuquerque, New Mexico.

Peng, H., & Tomizuka, M. (1993). Preview control of vehicle lateral guidance in highway automation. *Journal of Dynamic Systems, Measurement, and Control*, *115*, 679–685.

Pham, H., Hedrick, J. K., & Tomizuka, M. (1994). Combined lateral and longitudinal control of vehicles for IVHS. *Proceedings of the 1994 American control conference*, Vol. 2 (pp. 1205–1206), Baltimore.

Tan, H. S., Guldner, J., Chen, C., & Patwardhan, S. (1998). Changing lanes on automated highways with look-down reference systems. *Proceedings of the 1998 IFAC workshop on advances in automotive control* (pp. 69–74), Loudonville, OH, USA.